



Check for updates

AUTHORS:

Moshe G. Mosotho^{1,2}
Roelf D. Strauss¹
Rendani R. Ndanganeni²
Jacobus P. van den Berg^{1,2}

AFFILIATIONS:

¹Centre for Space Research,
North-West University,
Potchefstroom, South Africa
²Space Science Division,
South African National Space Agency,
Hermanus, South Africa

CORRESPONDENCE TO:

Moshe Mosotho

EMAIL:

mosothomoshegodfrey@gmail.com

DATES:

Received: 30 Oct. 2019

Revised: 25 Feb. 2020

Accepted: 13 June 2020

Published: 29 Jan. 2021

HOW TO CITE:

Mosotho MG, Strauss RD,
Ndanganeni RR, van den Berg
JP. The North-West University's
High Altitude Radiation Monitor
programme. *S Afr J Sci.*
2021;117(1/2), Art. #7561. [https://
doi.org/10.17159/sajs.2021/7561](https://doi.org/10.17159/sajs.2021/7561)

ARTICLE INCLUDES:

- Peer review
 Supplementary material

DATA AVAILABILITY:

- Open data set
 All data included
 On request from author(s)
 Not available
 Not applicable

EDITOR:

Amanda Weltman

KEYWORDS:

radiation, atmosphere, dose rate,
aircraft, public awareness

FUNDING:

South African National Space
Agency, South African National
Research Foundation, South African
National Astrophysics and Space
Science Programme

The North-West University's High Altitude Radiation Monitor programme

Since the discovery of cosmic radiation by Victor Hess in 1912, when he reported a significant increase in radiation as altitude increases, concerns about radiation effects on human bodies and equipment have grown over the years. The secondary and tertiary particles which result from the interaction of primary cosmic rays with atmospheric particles and commercial aircraft components, are the primary cause of the radiation dose deposited in human bodies and in electronic equipment (avionics) during aircraft flights. At an altitude of about 10 km (or higher) above sea level, the dose received by frequent flyers, and especially flight crew, is a serious concern. Also of concern is the possible failure of sensitive equipment on board commercial aircrafts as a result of flying through this mixed radiation field. Monitoring radiation in the atmosphere is therefore very important. Here we report on the first measurements by the High Altitude Radiation Monitor (HARM) detector during a commercial flight from Johannesburg (O.R. Tambo International Airport) to Windhoek (Hosea Kutako International Airport). As part of a public awareness activity, the HARM detector was placed on a high-altitude balloon, and these measurements are also shown here. Model calculations (estimations) of radiation levels for the commercial aircraft flight are shown and the results are used to interpret our measurements.

Significance:

- Measurements of the Regener–Pfozter maximum in South Africa and dosimetric measurements on board a commercial flight are presented.
- These radiation measurements are compared to model calculations which can be used to predict the radiation dose during commercial flights.
- This study also aims to raise public awareness about the atmospheric radiation environment from ground level to the Regener–Pfozter peak at high altitude.

Introduction

Earth is continuously exposed to ionising radiation from high-energy particles originating from galactic sources such as active galactic nuclei or supernova remnants¹⁻³, the Sun⁴ and particles trapped in the Van Allen radiation belts^{5,6}. Galactic and solar particles are energetic enough to interact with the Earth's atmosphere where they produce high-energy secondary particles. During commercial aircraft flights, these primary and secondary high-energy particles interact with aircraft components to further produce more high-energy secondary particles. Scientists have been assessing the exposure of crew members and commercial aircraft passengers to ionising radiation ever since it was identified as a health risk in the 1920s⁷, and since then, progress has been made over the years in measuring and monitoring radiation at flight altitudes^{8,9}. When exposed to radiation from these high-energy particles, the time-dependent amount of energy absorbed by human bodies, referred to as the dose rate, can be harmful because it can damage the body's DNA make-up.^{10,11} Even though our bodies are capable of repairing this damage, errors can occur during the repair processes, leading to a mutation of cells that can potentially result in cancer.^{12,13} Therefore, measurements of these secondary particles can be of help to improve our knowledge and understanding of post-exposure effects and thereby also improve the risk estimation for commercial aircrafts.

The production of secondary particles in the upper atmosphere is at a maximum rate¹⁴ at an altitude reported to be between 14 km and 20 km above sea level. This maximum altitude of ionising radiation is known as the Regener–Pfozter maximum (RP-max).¹⁵ The RP-max varies with geomagnetic (omnidirectional) cut-off rigidity, air pressure, and solar cycle activity and there is no fixed altitude position above sea level to represent it. Below this altitude, the intensity of secondary radiation steadily decreases due to absorption and decay processes.^{16,17} Therefore, to measure and monitor radiation exposure, at least up to the RP-max, a small, portable and lightweight instrument known as the High Altitude Radiation Monitor (HARM) was used. This acronym was used to honour the late Prof. Harm Moraal, who was part of the North-West University's (NWU) physics department for 44 years and championed cosmic ray research in South Africa. This instrument uses a Geiger–Müller (GM) counter, capable of detecting secondary and tertiary particles, and a number of smaller sensors added to provide additional information.

The South African National Space Agency's (SANSA) Space Science Division operates a wide range of infrastructure, all dedicated to studying the atmosphere, the Earth's magnetic field, the Sun, and the near-space environment. The agency's ground-based instruments are located across southern Africa and in Antarctica. For years, SANSA has been conducting real-time monitoring and forecasting of space weather events (<http://spaceweather.sansa.org.za>). Recently, the agency was selected by the International Civil Aviation Organization (ICAO) as one of two regional centres to provide space weather services, including solar storm forecasts and warnings, to the aviation industry from 2022. By the end of 2018, the ICAO had recommended that all flight plans must include space weather information by law.¹⁸ In anticipation of this, the HARM programme was initiated to characterise the radiation environment above South Africa at aviation altitudes. Here we report on the first HARM measurements

© 2021. The Author(s). Published
under a Creative Commons
Attribution Licence.

(and the model estimates) during a commercial aircraft flight and the measurements obtained during a high-altitude balloon launch.

Cosmic rays in the atmosphere

Cosmic rays are energetic charged particles, consisting mostly of protons, which can be classified into four main species, namely solar energetic particles (SEPs), anomalous cosmic rays, Jovian electrons (which are produced in the Jovian magnetosphere), and galactic cosmic rays (GCRs). However, only the GCR and SEP species are of importance here. The SEPs originate from the Sun and are accelerated mainly by solar flares, coronal mass ejections, and shocks in the interplanetary medium. The source of the GCRs is, however, located outside the region of space influenced by the solar wind and the solar magnetic field, known as the heliosphere¹⁹, in astrophysical sources such as supernova remnants¹⁻³. As they enter the heliosphere with energies of up to 10^{12} GeV²⁰, these particles interact with the solar wind and the embedded heliospheric magnetic field, causing their intensities to change as a function of time, position, and energy in a process called cosmic ray modulation.²⁰ This process is classified based on the timescale in which it occurs, i.e. short-term (from hours to days⁴), medium-term (from days to about a month and sometimes more than that²¹), and long-term (from a month to years or decades and even beyond) modulation effects.

The level of modulation greatly depends on the energy of these particles. At Earth, cosmic rays are denied free access to the ground level due to the orientation of the geomagnetic field. Therefore, depending on their energies (or rigidity, which defines a measure of the momentum of the particle per elementary charge), their arrival direction, and the period of solar activity, these particles can be deflected back into space, get trapped in the geomagnetic field, or they can penetrate and make their way to the top of the atmosphere.

For vertically incident particles originating from space, it is easy for particles with both high and low energies to penetrate the geomagnetic field at the polar regions because the geomagnetic field lines are directed perpendicular to the surface, leading to higher fluxes in these regions. In a geocentric dipole field, geomagnetic cut-off rigidity is defined as the minimum momentum per charge a particle must have in order to reach a specific position, given a certain arrival direction.²² Throughout this article, we use the geomagnetic cut-off rigidity of a particle with vertical incidence, labelled P_c . At Earth, P_c varies from 0 GV at the geomagnetic polar regions to about 17 GV in the mid-latitudes. Due to the more effective shielding at the mid-latitude regions, fewer particles can reach the ground level at mid-latitudes.^{22,23}

As primary GCRs and SEPs penetrate the geomagnetic field and traverse down to lower altitudes they will interact with the atmospheric particles, producing secondary particles such as neutrons, protons and electrons. A simplified schematic (not drawn to scale) illustrating the primary cosmic ray interaction with the upper atmosphere which results in a cascade of secondary particles is shown in Figure 1. This cascade continuously occurs until the particles lose all their energy and are finally absorbed in the lower atmosphere.²³ For a cosmic ray particle to sustain an atmosphere cascade which is observed at ground level, the primary particles need at least 1 GV in rigidity.

To study the behaviour of secondary cosmic rays on both long and short timescales, neutron monitors (NMs) are the most preferred detectors. NMs have been observing cosmic ray activity since 1951 when J.A. Simpson built the first monitor.²⁴ They measure the secondary particles' by-products, mainly neutrons and protons.²⁵ The four chosen NMs considered here are located in Antarctica (at the South African research base, SANAE), South Africa (Hermanus and Potchefstroom) and Namibia (Tsumeb), at cut-off rigidities (altitudes) ranging from about 0.86 GV (0.052 km) in Antarctica to about 9.15 GV (1.240 km) in Namibia. They are all operated by the Centre for Space Research of the NWU. The Centre has been involved with these types of observation in the southern hemisphere for over 60 years since the late 1950s.

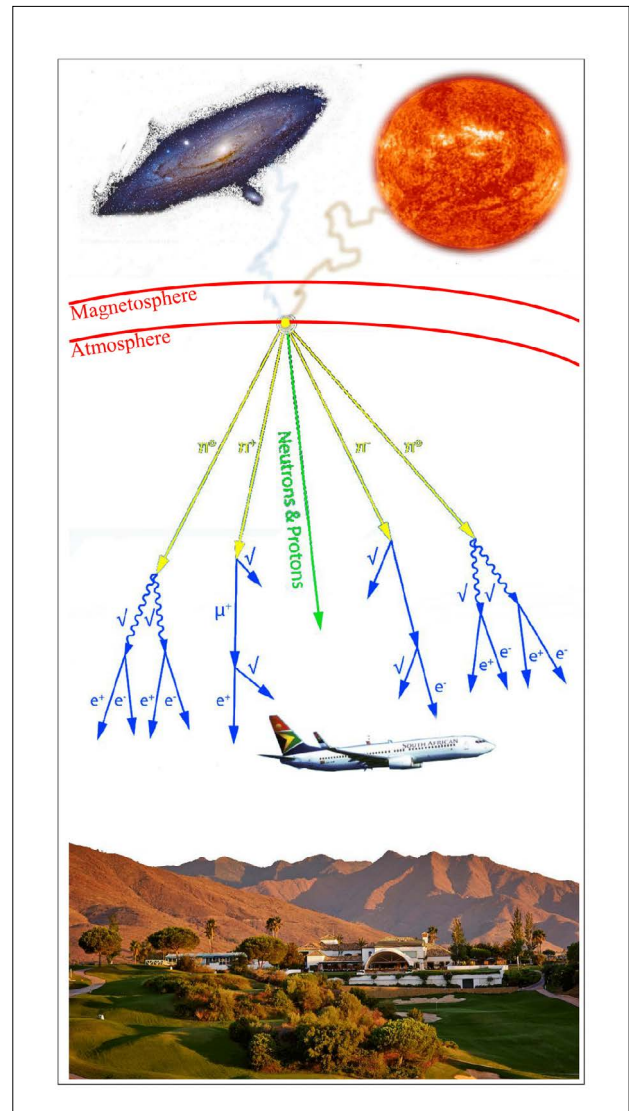


Figure 1: Basic representation of the cosmic ray cascade. The figure is not to scale.

Figure 2a shows the long-term cosmic ray NM count rates as a function of time, with all the NMs normalised to 100% in March 1987. Clearly, from this long-term record, NMs react to modulation based on P_c . A monitor with a lower P_c , i.e. SANAE at 0.86 GV, will be more sensitive to modulation and record higher count rates than a monitor with higher P_c , i.e. Tsumeb at 9.15 GV. Apart from detecting the secondary particles' by-products, NM counts on the ground can also give an indication of the primary cosmic ray flux at and above the top of the atmosphere.

In contrast to the quasi-constant quiet-time GCR levels, the Sun can produce short-term transient increases of cosmic rays at the ground level. These ground-level enhancements (GLEs) are caused by relativistic SEPs²⁶ being accelerated in solar flares and coronal mass ejections. These SEPs have sufficient intensity and energy to greatly enhance the atmospheric secondary radiation environment.²⁷ The first GLE was registered on 28 February 1942, and only 72 GLEs have occurred to date. Note that these solar transient events can also modulate the GCR levels over longer timescales.

Figure 2b shows the percentage increase measured by the four chosen NMs during the GLE of 29 September 1989, also referred to as GLE 42. This GLE is the only one for which all four NMs simultaneously registered a significant increase. The SANAE NM registered a 297.5% peak increase, while the Hermanus, Potchefstroom and Tsumeb NMs recorded 105.1%, 105.3% and 62.2% increases, respectively. A GLE can therefore lead to increases in the NM count rate of several orders of magnitude.

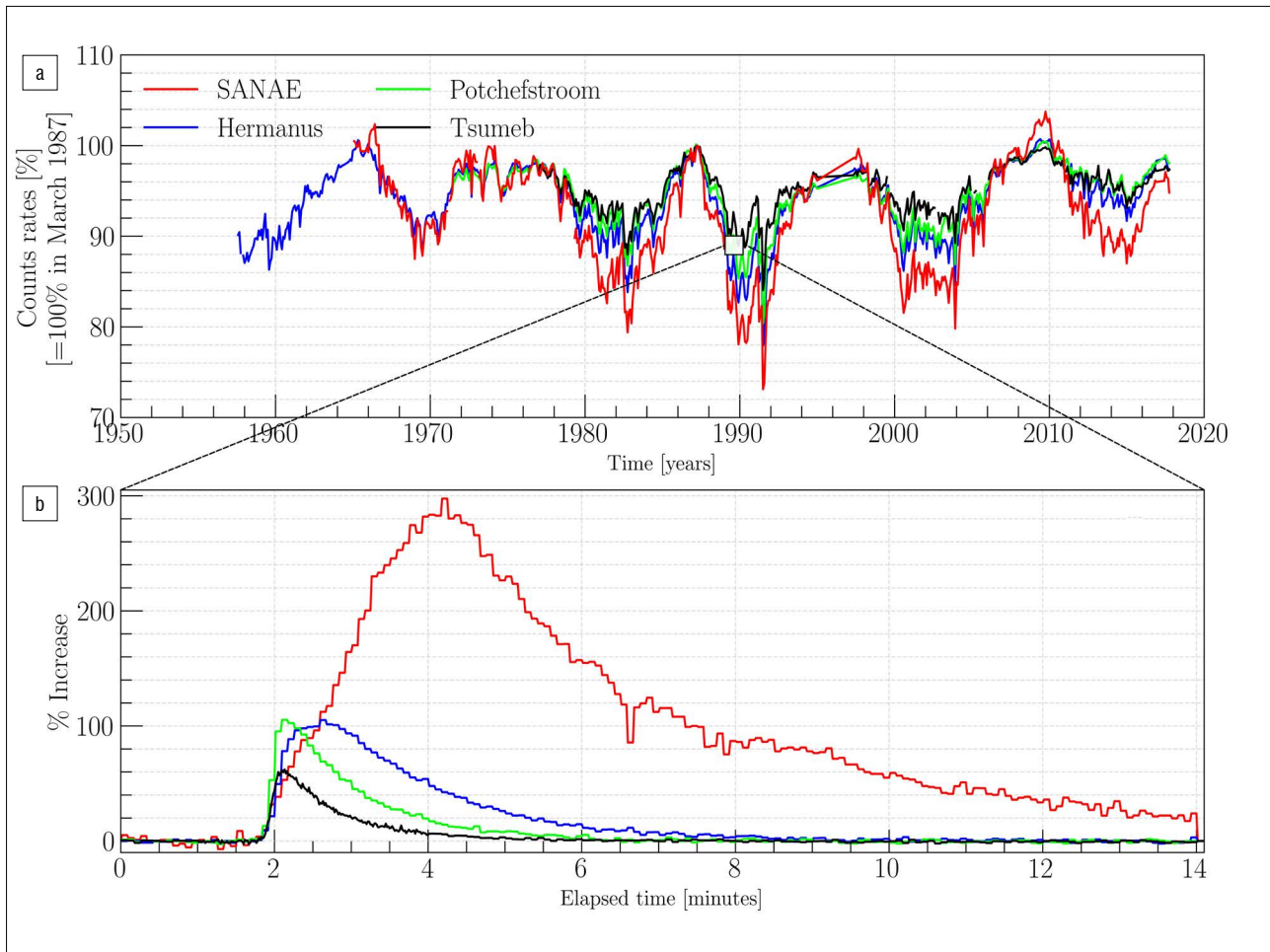


Figure 2: (a) Long-term and (b) short-term neutron monitor count rates observed by the four chosen neutron monitors. The data were taken from: <http://natural-sciences.nwu.ac.za/neutron-monitor-data>.

The High Altitude Radiation Monitor programme

The HARM programme is a student's project initiated by the NWU's Centre for Space Research. This programme offers opportunities for students to conduct technological and scientific experiments related to cosmic radiation in the atmosphere.

The HARM is a compact, battery-powered detector, which records cosmic radiation levels and is based on a Raspberry Pi micro-computer discussed below. The HARM prototype has been used to take measurements on board commercial aircrafts at aviation altitudes and also during high-altitude balloon launches. The balloon measurements allow the monitoring of the atmospheric radiation environment from ground level to high altitudes (in principle up to 40 km). These measurements of secondary and tertiary particles give information about the atmospheric radiation environment's evolution with altitude. The programme has been made available to students from other institutions through a collaboration with SANSA. Figure 3 shows students taking part in the HARM programme. Figure 3a shows Phillip Heita and Jacobus van den Berg from the NWU pictured with the first HARM prototype, while Figure 3b shows Portia Legodi from the University of Cape Town assembling an upgraded version of the HARM prototype, and Figure 3c shows Chris Thaganyana (pictured holding the inflator system nozzle and the balloon neck) from the University of the Western Cape taking part in the first HARM balloon launch.

The importance of this programme is to impart knowledge to the general public about the atmospheric radiation environment's evolution when flying, relative to altitude, geomagnetic position, solar activity, and flight duration. Apart from that, this programme assists students in gaining

experience in designing, testing, and assembling relatively simplistic instruments to make novel measurements.

Instrumentation

Figure 4 shows the instruments comprising the basic detector system. All the sensors and modules are self-contained and draw their power directly from the Raspberry Pi computer which is powered with a standard power bank. For this particular HARM set-up, the following components were used:

- The Raspberry Pi 3 Model B+ micro-computer. This compact computer board offers endless opportunities for student projects. It is easy to add different sensors to this board, which can be programmed relatively easy. For more details, see <https://www.raspberrypi.org/>.
- The Raspberry Pi Sense HAT. The sensor measures environmental parameters such as pressure, temperature, humidity, acceleration and the magnetic field magnitude. These parameters are sampled once per minute.
- The J305 β GM counter. The tube is cylindrical and capable of sensing low-energy ionising radiation. However, the counter will not normally detect neutrons as these do not ionise the gas inside the tube. The tube is powered from the Raspberry Pi by a radiation board from [cooking-hacks.com](https://tinyurl.com/ox76ha5) (<https://tinyurl.com/ox76ha5>). The board also discretises the GM counters' pulses, which is read by the Raspberry Pi.
- All components are housed in a 3D-printed housing.

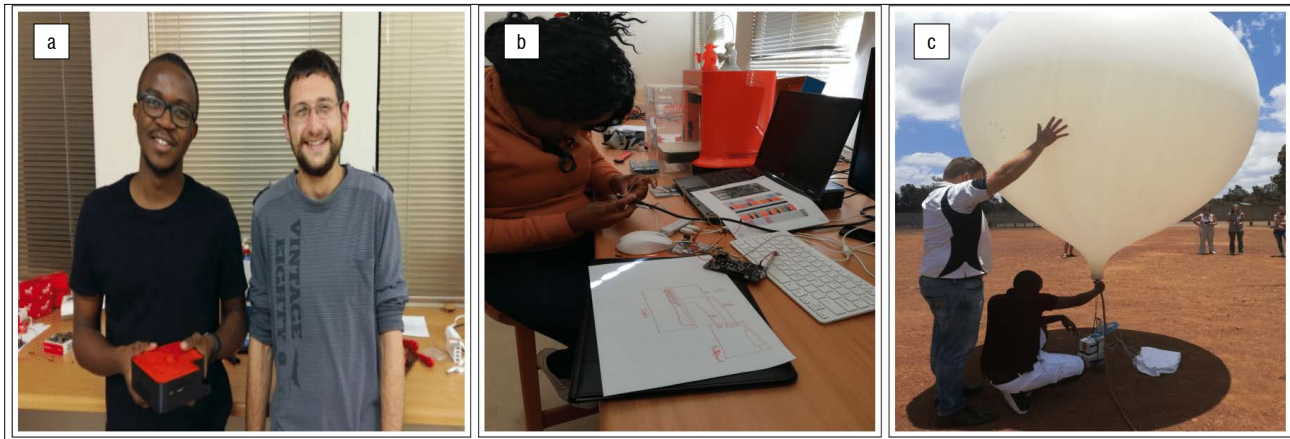


Figure 3: Students participating in the HARM programme. These activities occurred in the following order: (a) in June 2017 the first HARM prototype was assembled, (b) in June 2018 the prototype was upgraded and (c) in November 2018 the first HARM balloon launch took place.

The whole HARM set-up uses less power than a standard laptop, and does not radiate any high-frequency signals (all wireless connections, such as Bluetooth, are disabled). The detector can thus be safely used on board commercial flights. To fulfil several requirements to conduct more projects (including balloon launches), HARM has undergone several iterations resulting in different set-ups since the first version pictured in Figure 4. To reduce mass, the Raspberry Pi Model B+ was replaced with a smaller Raspberry Pi Zero W, while the Sense HAT was replaced with a BMP180 barometric pressure sensor. A real-time clock was added to keep the time, while a camera module was added for balloon launches. A camera was mounted outside a Styrofoam box to take pictures of the landscape and sky during the flight.

High-altitude balloon flight measurements

Aside from the scientific consideration, there is much more to be taken into consideration, such as applying for permission to launch the balloon from the Air Traffic and Navigation Services (ATNS) (<https://www.atns.com/>) – an entity of the South African Department of Transport. Prior to launching, the following equipment must be available: a meteorological rubber balloon, helium/hydrogen gas, an insulated payload box, detection system, location mapping tracker, and a parachute. All the instruments used are mounted inside, except the camera. The detector is tracked by placing a smartphone inside the box and using the standard tracking software of the phone.

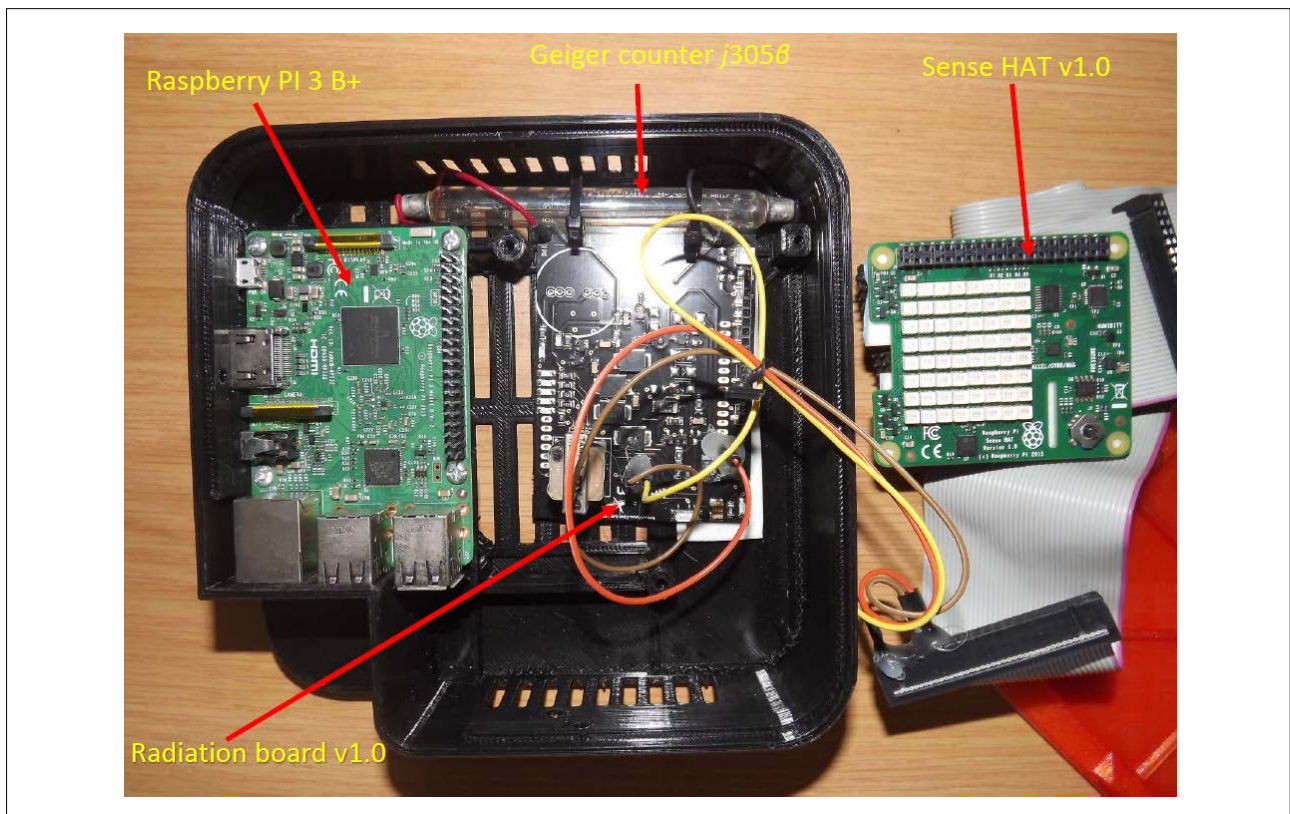


Figure 4: The HARM housing opened to reveal the detector electronics, showing the Raspberry Pi 3 Model B+, the GM tube and its control board, and the Sense HAT v1.0.

Launch site, burst altitude and landing site

To predict and estimate the flight path, burst altitude and landing site, this online website <http://www.habhub.org> can be useful. This process must be done a couple of days before the launch day. Once the launch site is chosen and the payload assembled, the ATNS can be contacted to apply for permission to launch the balloon.

For the recent balloon launch, a 1-kg natural rubber balloon was used. It was inflated with just enough helium gas to lead to a neck lift of about 1 kg. It was inflated until the payload and weights were lifted. With a payload ranging from about 1 kg to about 1.5 kg, the balloon was expected to produce an ascent rate ranging from about 5.5 m/s to 6.0 m/s. The balloon rises unguided and after reaching the burst altitude, the balloon bursts, and the payload returns to Earth with the help of a parachute of about 2.5 m in diameter. The descent rate of the balloon was estimated to range between about 7.5 m/s and 8.0 m/s as the payload approached the ground. The total duration of the flight was expected to be less than 5 h, depending on the wind patterns and weather conditions from the launch site to the burst altitude and back to the ground.

Figure 5 shows a summary of the high-altitude balloon launch. Figure 5a shows a balloon being prepared for launch, while Figure 5b shows a snapshot of the sky and the Earth horizon. Figure 5c shows the remains

of a high-altitude rubber balloon just after it burst. Figure 5d shows the retrieved payload, at a distance from the launch site further than the predicted landing location, in an empty field.

The Model for Atmospheric Ionising Radiation Effects

The Model for Atmospheric Ionising Radiation Effects (MAIRE) from the RadMod Research Group was used in this work. MAIRE is a parameterised model based on particle transport calculations in the atmosphere using the FLUKA Monte Carlo code. The model is capable of calculating particle fluxes of different species using an incident GCR or SEP input spectrum at least up to an altitude of 100 km above sea level. These fluxes can be calculated for any desired date, geographic/geomagnetic flight position and solar activity. The simulated fluxes can then be used as an input parameter to calculate dose rates (in $\mu\text{Sv/h}$) and accumulated doses (in μSv) for commercial aircrafts or for stratospheric radiation balloon measurements. The other calculation that can be taken into consideration is the possibility of a GLE occurring during the flight. These calculated values can then be used to compare with measurements obtained using a dosimeter. Currently, the model can be accessed only through the website www.radmod.co.uk/maire, due to the unavailability of its source code.

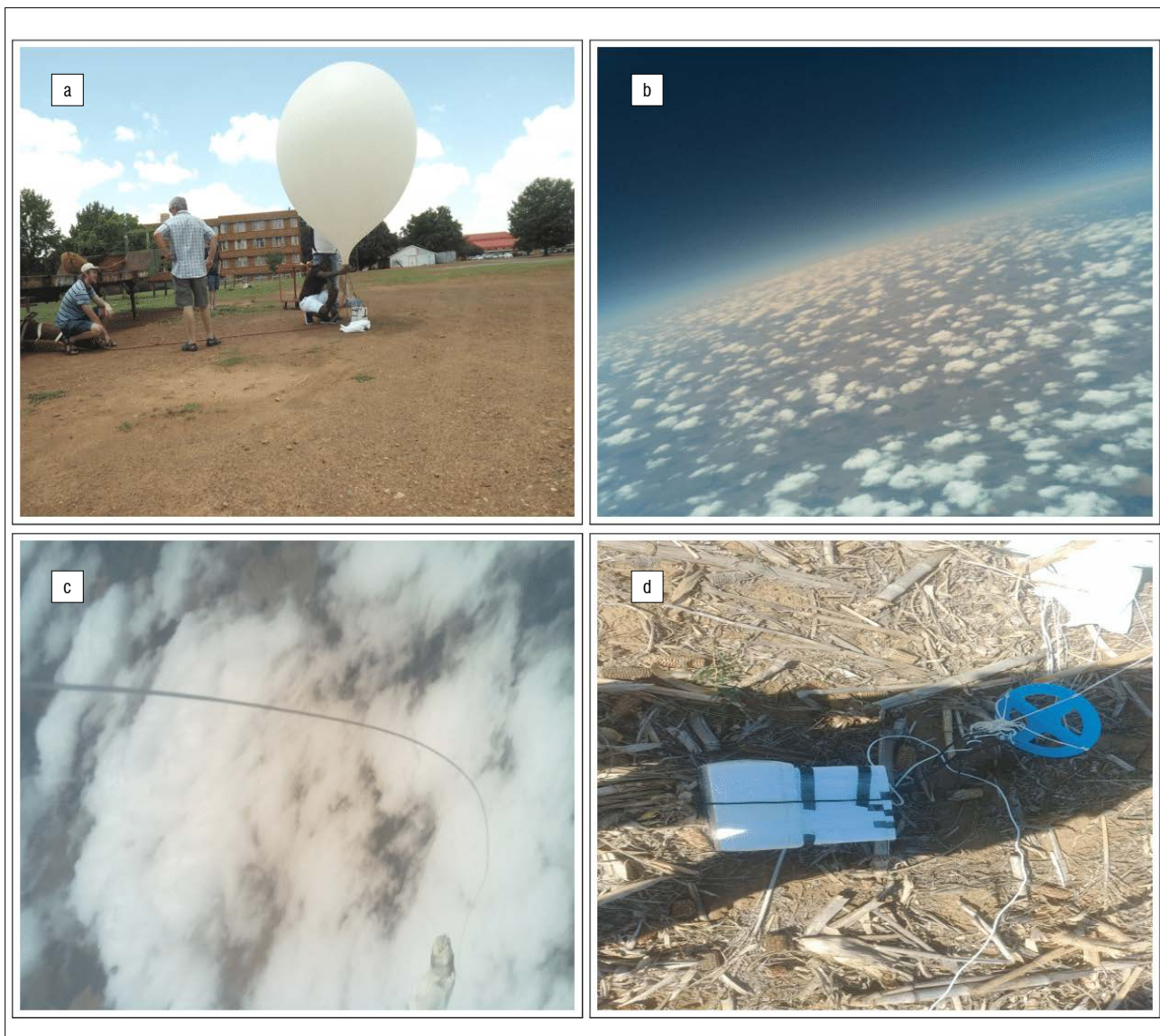


Figure 5: High-altitude balloon launch: (a) launch site, (b) Earth horizon, (c) the burst balloon captured during the descent, and (d) landing site.

Results and discussion

Measurements on board an aircraft

The measurements obtained during the first commercial flight of HARM are discussed below. The measured count rates are compared with the model calculations for the same date. Figure 6 shows the measured and calculated results.

In Figure 6a, the measured quantities are shown as a function of the elapsed time from departure. The count rates on board just before take-off and just before landing were not recorded as the device was switched off (see grey shaded areas) as requested by the aircraft flight personnel. The scattered error bar for each measurement was calculated as a Poissonian error. A 2-min moving average of the data (red solid line) was taken to show a smooth data trend. However, despite the shielding provided by the atmosphere, the HARM count rates rapidly increased above the background cosmic ray levels at ground level after take-off and levelled off at the cruising altitude recording count rate of between 25 per minute and 35 per minute, until the descent started before landing. The average value of the measured count rate at the cruise altitude was about 29 per minute.

Ideally, the first step of comparing the count rate measurements with model calculations is to use data sets acquired for the same date and time. These measured data sets must include information on the geographic flight position as well as corresponding measurements of at least one dosimetric parameter, e.g. the effective dose or ambient dose. However, because the HARM is unable to directly measure any dosimetric quantities (a GM counter produces only a count rate which cannot be related to a dosimetric quantity in a mixed radiation field), the data and model were compared in a qualitative fashion only. From Figure 6, the model results (blue solid line) show a general agreement with the count rate data (red scattered data), as measured by HARM, within some uncertainties.

The individual dose limit for members of the general public is 1 mSv/year (or an average dose rate of about $0.115 \mu\text{Sv/h}$ over a year). However, if this limit is exceeded in a working environment (e.g. for nuclear plant workers), workers are classified as radiation workers, whose average dose limit is set to be 20 mSv/year (or an average dose rate of about $2.289 \mu\text{Sv/h}$; <http://www.nnr.co.za/>). Using the estimated doses from the model, the average effective dose rate from O.R. Tambo International Airport to Hosea Kutako International Airport is about 10 km above sea level for a duration of about 80 min, while the

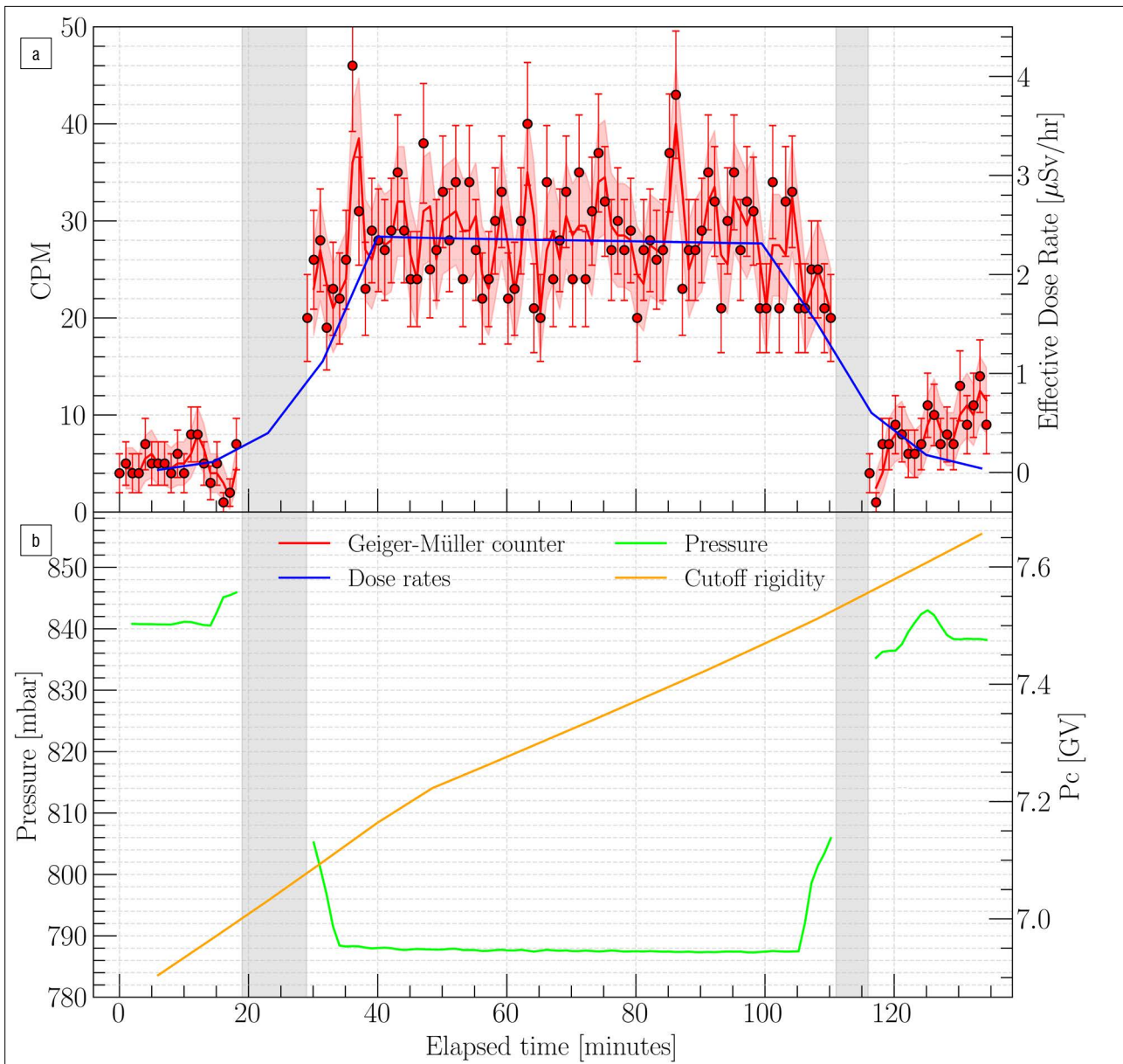


Figure 6: (a) The counts per minute (CPM; red colour) and model dose rates profile (blue colour). (b) Sensor HAT barometric pressure (green colour) and the P_c profile (orange colour).

HARM measured count rate is 29 per minute, on average. For an average member of the public, taking only several flights a year, the radiation exposure from flying is therefore negligible. However, if an aircrew member flies at least 285 short-haul flights per year (six such flights per week), using the same flight path and about the same flight time, they would receive a dose rate greater than 1 mSv/year – higher than the radiation exposure limit for the general public. This finding illustrates the need to define aircrew as radiation workers. These assumptions would be more realistic if the atmospheric conditions were the same, i.e. if there were no SEP events which might greatly enhance the atmospheric secondary radiation environment at cruising altitudes. In fact, aircrew in Germany have been classified as radiation workers as defined in the Radiation Protection Ordinance (StrlSchV) ²⁸, while the German Federal Radiation Registry documents individual monthly effective doses for all aircrew members²⁹. This is currently not the case in South Africa.

In Figure 6b, the aircraft cabin pressure profile is as expected when compared with the count rate profile: As the cabin pressure inside the aircraft changes due to the outside pressure changing, it directly corresponds to variations in altitude. As seen from Figure 6b, before take-off a small increase in pressure is expected when the cabin door closes and similarly when the cabin door opens after landing a small decrease is observed in the pressure profile. During take-off, because the detector was switched off for about 10 min, it appears that cabin pressure started rapidly decreasing and it levelled off at the cruising altitude, recording an average cabin pressure of about 787 mbar. Also shown in Figure 6b is the Pc profile from the MAIRE model calculation changing from 6.904 GV at O.R. Tambo International Airport to 7.656 GV at Hosea Kutako International Airport.

Measurements onboard a stratospheric balloon

Since the 1950s, an interest in observing cosmic ray particles through experiments with high-altitude balloons has been re-ignited³⁰ in the NM era. Among other discoveries made from these balloon launches, the most recent and notable is the disappearance of the RP-max by Hands and colleagues³¹ using a low-cost portable radiation monitor. In South Africa, high altitude radiation dosimetry studies from ground level have not been documented before. However, the NWU (then known as Potchefstroom University for Christian Higher Education) conducted undocumented balloon launches for 20 years between 1958 and 1978 which characterised radiation levels with respect to ground level. Therefore, to address the unquantified and undocumented radiation levels, a balloon carrying the HARM instruments was launched at the NWU's Potchefstroom campus on 29 November 2018 after verifying in the laboratory that HARM's detection system was working and that all data were being received and recorded. The launch was successful and the measurements made by HARM are presented in Figures 7 and 8. The Pc at the launch site was 6.88 GV and at the landing site was 7.03 GV. These cut-off rigidities were calculated using the International Geomagnetic Reference Fields 2010 model.

From Figure 7, the profiles of the measurements, i.e. the count rate and atmospheric pressure and temperature, are plotted as a function of the elapsed time from launch. In both panels, the red and blue colours represent the ascend and descend phases, respectively, while the grey shaded area represents the burst altitude area. The red and blue vertical shaded areas in the ascend and descend phases represent the measurements at the aircraft cruising altitude between 10 km and 12 km. The count rate profile is shown in Figure 7a. The solid line represents a

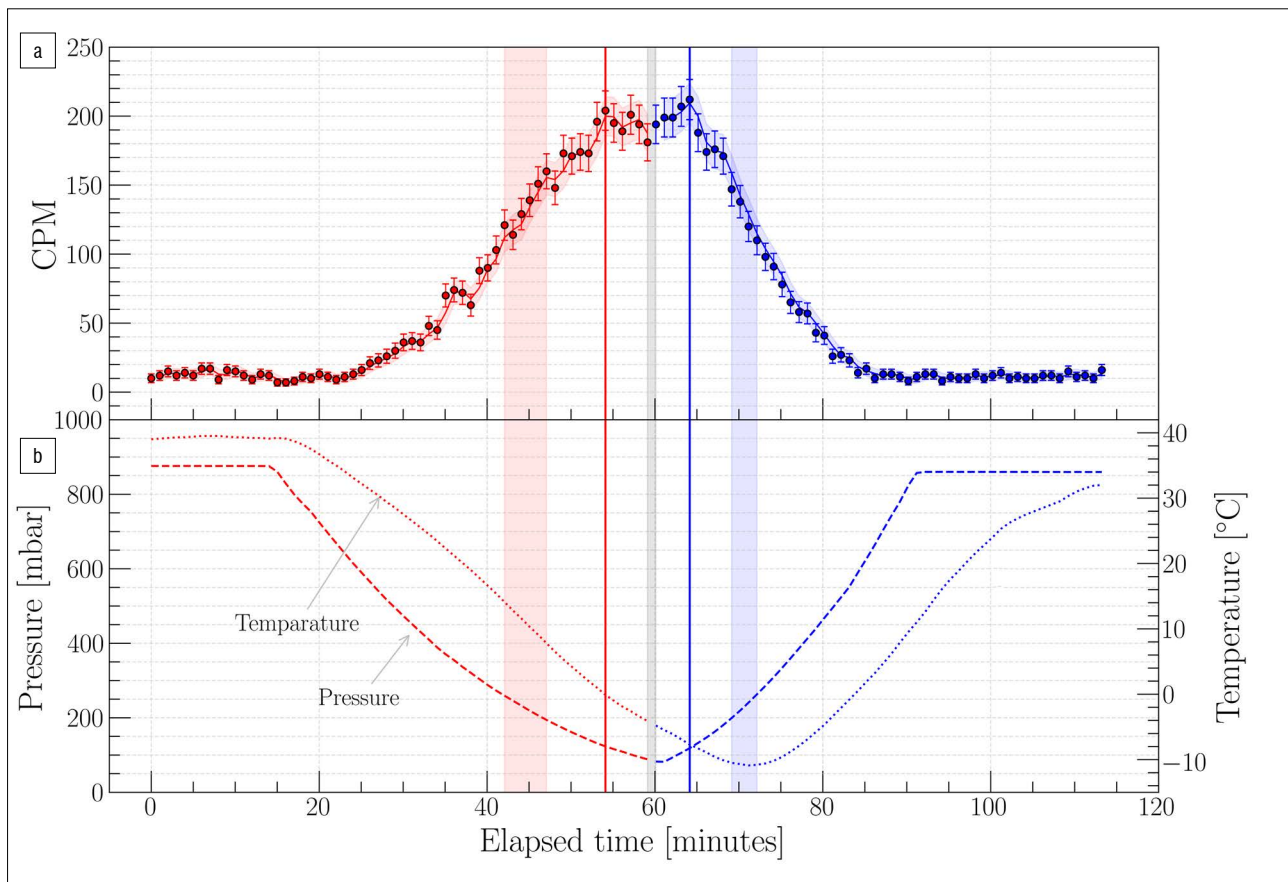


Figure 7: (a) The counts per minute (CPM) and (b) atmospheric pressure and temperature are shown as a function of the elapsed time from launch. The red and blue colours represent the ascend and descend phases, respectively, while the grey shaded area represents the burst altitude area. The red and blue vertical shaded areas in the ascend and descend phases represent the measurements at the aircraft cruising altitude between 10 km and 12 km. The blue and red thin vertical lines represent the RP-max before and after the burst altitude, respectively.

2-min running average, while actual measurements are shown in the original 1-min resolution as circles. At an ascent rate of 6.0 m/s from the launch site, it took the balloon about 27 min to reach the 10-km cruise altitude of commercial aircrafts. Clearly, from the shaded region in the ascent and descent phases, the balloon spent less time at the cruise altitude during the descent phase than it did in the ascension phase. Also seen from these data is what appears to be peaks, marked by the blue and red thin vertical lines during the ascent and descent phases. These peaks before and after the burst altitude are known as the RP-max. The profile of the measured atmospheric pressure and temperature, as a function of the elapsed time from launch, is shown in Figure 7b. The measured atmospheric pressure decreased as the count rate profile started increasing to high altitudes, as expected. At commercial flight altitudes, the pressure measured was between 200 mbar and 300 mbar, during both ascension and descension. The lowest recorded pressure and temperature was 82 mbar and $-11\text{ }^{\circ}\text{C}$ at the burst altitude (at the cruise altitude during the descent phase).

Figure 8 shows the correlation between the measured count rate and altitude. As pressure was measured using the BMP180 barometric pressure sensor and it is well known that pressure varies with altitude, the measured pressure from the sensor can be used to calculate an approximate measure of altitude. To approximate this altitude, an international barometric formula was used³², which takes into account the average sea level pressure and the local pressure above sea level, and outputs an altitude value above sea level. The count rates were plotted together with the approximate altitude values. The shaded region between the 10-km and 12-km altitudes shows the count rate values at commercial flight cruise altitudes. At altitudes of about 14.7 km and 14.9 km, the count rate profile during ascent and descent phases shows clear peaks. These peaks seem to represent the RP-max.

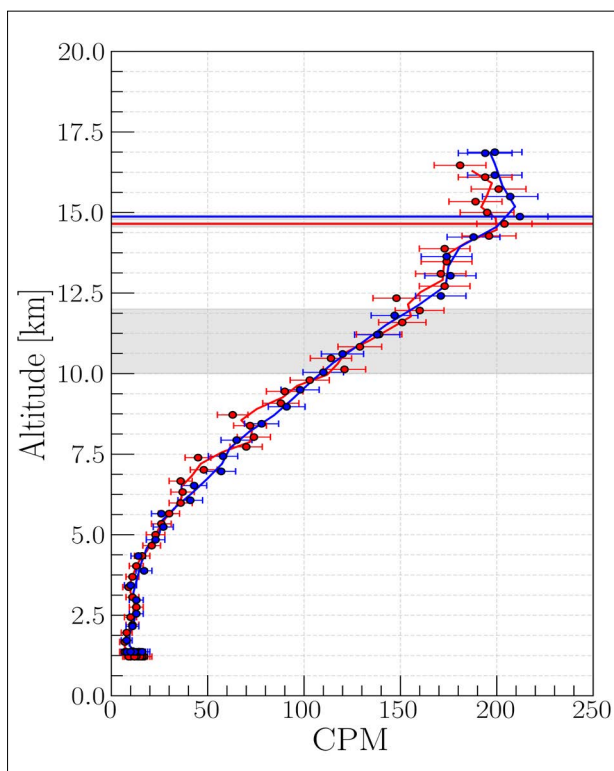


Figure 8: The counts per minute (CPM) profile of the balloon flight shown as a function of altitude. Red represents ascent, while blue represents descent. The grey shaded area between 10 km and 12 km represents the expected count rate measurement at the aircraft cruising altitude, while the horizontal lines at about 14.9 km and 14.7 km show the count rate measurements at the RP-max before and after burst altitude.

Conclusions

The biggest advantage of using the HARM prototype was that it is relatively low cost. Most of the components contained inside are off the shelf and only require knowledge of Python programming and rudimentary knowledge of sensor electronics. During balloon launches, most of the payloads used are recoverable, making it even more affordable and easy to relaunch using the same payload. The HARM programme has succeeded in measuring the mixed radiation field with respect to the geographic flight position during commercial aircraft flights and stratospheric balloon launches. These data sets are of interest to atmospheric scientists, space weather forecasters, commercial and private aircraft crew, and, most importantly, for public awareness. In principle, it is possible to obtain data every day and even during rare events like the SEP events from the ground up to the RP-max.

The HARM's first measurements of the RP-max and aviation radiation measurements on board a commercial flight in South Africa were presented. There is, however, room for improvement in these measurements. For one thing, the GM counter fails to measure the amount of energy being deposited by these particles upon contact with the tube. They also have a very poor response to neutrons. However, the inexpensive nature of the HARM detector and the relative ease of adding sensors to a Raspberry Pi micro-computer, make this an ideal student project. From the measurements obtained using HARM's GM counter it is not possible to calculate the dose rate. Therefore, the RPiRENA prototype, based on silicon semiconductor sensors, is being designed, in conjunction with researchers at the University of Kiel in Germany.^{8,9}

As the only Space Weather Warning Centre in Africa, SANSA's appointment by ICAO as one of two regional centres to provide space weather services and warnings is a big boost for space science research in South Africa. As recommended by ICAO, SANSA must provide radiation estimates to the aviation sector, and the HARM programme can not only assist with this task, but also with raising public awareness regarding radiation levels at aviation altitudes.

Acknowledgements

We thank the students and researchers who participated in the HARM programme, from assembling the HARM prototypes to voluntarily carrying them on board aircrafts and taking measurements. We are especially grateful to Phillip Heita, Portia Legodi, Chris Thaganyana, Wessels Reitsma, and Gunther Drevin. We gratefully acknowledge the reviewers' valuable suggestions that improved the quality of the manuscript. Finally, we thank the North-West University and the South African National Space Agency for their collaborative effort in promoting high altitude radiation studies. We acknowledge financial support from the South African National Space Agency, the South African National Research Foundation, and the South African National Astrophysics and Space Science Programme.

Authors' contributions

G.M.M.: Conceptualisation, methodology, data collection, data analysis, writing – the initial draft, writing – revisions. R.D.T.S.: Conceptualisation, methodology, writing – revisions, student supervision, project leadership, funding acquisition. R.R.N. Methodology, writing – revisions, funding acquisition. P.J.v.d.B.: Conceptualisation, writing – revisions.

References

1. Ackermann M, Ajello M, Allafort A, Baldini L, Ballet J, Barbiellini G, et al. Detection of the characteristic pion-decay signature in supernova remnants. *Science*. 2013;339:6121. <https://doi.org/10.1126/science.1231160>
2. Ginzburg VL, Syrovatskii SI. Origin of cosmic rays. *Geomagn Aeron*. 1961;1:427.
3. Hillas AM. Cosmic rays: Recent progress and some current questions. *arXiv*. 2006. <https://arxiv.org/pdf/astro-ph/0607109.pdf>
4. Forbush SE. Three unusual cosmic-ray increases possibly due to charged particles from the Sun. *Phys Rev*. 1946;70:771–772. <https://doi.org/10.1103/PhysRev.70.771>



5. Van Allen JA. Observation of high intensity radiation by satellites 1958 alpha and gamma. *J Jet Propuls.* 1958;28:588–592. <https://doi.org/10.2514/8.7396>
6. Van Allen JA, Frank LA. Radiation around the Earth to a radial distance of 107,400 km. *Nature.* 1959;183:430–434. <https://doi.org/10.1038/183430a0>
7. US National Research Council Committee on the Biological Effects of Ionizing Radiation (BEIR V). Health effects of exposure to low levels of ionizing radiation: Beir V. Washington DC: US National Academies Press; 1990. <https://doi.org/10.17226/1224>
8. Möller T, Berger T, Böttcher S, Burmeister S, Ehresmann B, Heber B, et al. The calibration of the flight radiation environment detector (FRED). In: Proceedings of 33rd International Cosmic Ray Conference; 2013 July 2–9; Rio de Janeiro, Brazil. <https://doi.org/10.13140/2.1.1179.9046>
9. Ritter B, Maršálek K, Berger T, Burmeister S, Reitz G, Heber B. A small active dosimeter for applications in space. *Nucl Instrum Meth B.* 2014;748:61–69. <https://doi.org/10.1016/j.nima.2014.02.030>
10. Hellweg CE, Spitta LF, Koch K, Chishti AA, Henschenmacher B, Diegeler S, et al. The role of the nuclear factor kb pathway in the cellular response to low and high linear energy transfer radiation. *Int J Mol Sci.* 2018;19(8):2220. <https://doi.org/10.3390/ijms19082220>
11. Koch K. The role of nuclear factor kb in the cellular response to different radiation qualities [dissertation]. Cologne: University of Cologne; 2013
12. Hellweg CE, Baumstark-Khan C. Getting ready for the manned mission to Mars: The astronauts' risk from space radiation. *Naturwissenschaften.* 2007;94:517–526. <https://doi.org/10.1007/s00114-006-0204-0>
13. Wilson JW, Goldhagen P, Rafnsson V, Clem JM, De Angelis G, Friedberg W. Overview of atmospheric ionizing radiation (AIR) research: SST-present. *Adv Space Res.* 2003;32(1):3–16. [https://doi.org/10.1016/S0273-1177\(03\)90364-4](https://doi.org/10.1016/S0273-1177(03)90364-4)
14. Bazilevskaya GA, Krainev MB, Makhmutov VS. Effects of cosmic rays on the Earth's environment. *J Atmos Sol-Terr Phys.* 2000;62:1577–1586. [https://doi.org/10.1016/S1364-6826\(00\)00113-9](https://doi.org/10.1016/S1364-6826(00)00113-9)
15. Regener E, Pfozter G. Intensity of the cosmic ultra-radiation in the stratosphere with the tube-counter. *Nature.* 1934;134:325. <https://doi.org/10.1038/134325b0>
16. Gaisser TK, Engel R, Resconi E. Cosmic rays and particle physics. Cambridge: Cambridge University Press; 2016. <https://doi.org/10.1017/CBO9781139192194>
17. Grieder PKF. Cosmic rays at Earth: Researcher's reference, manual and data book. Amsterdam: Elsevier; 2001.
18. South African National Space Agency (SANSA). SANSA Policy brief: Space weather impacts on aviation [document on the Internet]. c2016 [cited 2020 Feb 25]. Available from: <https://tinyurl.com/y29ykjv7>
19. Parker EN. Dynamics of the interplanetary gas and magnetic fields. *Astrophys J.* 1958;128:664. <https://doi.org/10.1086/146579>
20. Parker EN. The passage of energetic charged particles through interplanetary space. *Planet Space Sci.* 1965;13:9–49. [https://doi.org/10.1016/0032-0633\(65\)90131-5](https://doi.org/10.1016/0032-0633(65)90131-5)
21. Alania MV, Modzelewska R, Wawrzynczak A. On the relationship of the 27-day variations of the solar wind velocity and galactic cosmic ray intensity in minimum epoch of solar activity. *Solar Phys.* 2011;270(2):629–641. <https://doi.org/10.1007/s11207-011-9778-6>
22. Bütkofer R. Cosmic ray particle transport in the Earth's magnetosphere. In: Malandraki O, Crosby N, editors. Solar particle radiation storms forecasting and analysis. Astrophysics Space Science Library vol. 444. Cham: Springer; 2018. p. 79–94. https://doi.org/10.1007/978-3-319-60051-2_5
23. Schlaepfer H. Cosmic rays (Spatium 11). Zürich: International Space Science Institute; 2003.
24. Simpson JA. The cosmic ray nucleonic component: The invention and scientific uses of the neutron monitor. *Space Sci Rev.* 2000;93(1):11–32. <https://doi.org/10.1023/A:1026567706183>
25. Clem J, Dorman L. Neutron monitor response functions. *Space Sci Rev.* 2000;93:335–359. <https://doi.org/10.1023/A:1026508915269>
26. Bazilevskaya GA. Solar cosmic rays in the near Earth space and the atmosphere. *Adv Space Res.* 2005;35:458–464. <https://doi.org/10.1016/j.asr.2004.11.019>
27. Lantos P. Radiation doses received on-board aeroplanes during large solar flares. *Hvar Observatory Bulletin.* 2003;27:171–178.
28. StriSchV. Verordnung über den Schutz vor Schaden durch ionisierende Strahlen [Ordinance on protection against damage caused by ionizing radiation. Koeln: International atomic energy agency; 2001. German.
29. Wollschläger D, Hammer GP, Schafft T, Dreger S, Blettner M, Zeeb H. Estimated radiation exposure of German commercial airline cabin crew in the years 1960–2003 modeled using dose registry data for 2004–2015. *J Expo Sci Environ Epidemiol.* 2018;28:275–280. <https://doi.org/10.1038/jes.2017.21>
30. Maurin D, Melot F, Taillet R. A database of charged cosmic rays. *A & A.* 2014;569:A32. <https://doi.org/10.1051/0004-6361/201321344>
31. Hands ADP, Ryden KA, Mertens CJ. The disappearance of the Pfozter-Regener maximum in dose equivalent measurements in the stratosphere. *Space Weather.* 2016;14:776–785. <https://doi.org/10.1002/2016SW001402>
32. Grigorie TL, Dinca L, Corcau J, Grigorie O. Aircrafts' altitude measurement using pressure information: Barometric altitude and density altitude. *WSEAS Trans Circuits Syst.* 2010;9:1109–2734. <https://dl.acm.org/doi/abs/10.5555/1865266.1865273>